MOLECULAR AND CELLULAR BIOLOGY, May 2010, p. 2498–2507 Vol. 30, No. 10
0270-7306/10/$12.00 doi:10.1128/MCB.00646-09

Functional Effects of *PTPN11* (SHP2) Mutations Causing LEOPARD Syndrome on Epidermal Growth Factor-Induced Phosphoinositide 3-Kinase/AKT/Glycogen Synthase Kinase 3β Signaling▽

Thomas Edouard,[1]† Jean-Philippe Combier,[1]† Audrey Nédélec,[1] Sophie Bel-Vialar,[3] Mélanie Métrich,[4] Francoise Conte-Auriol,[1,2] Stanislas Lyonnet,[5] Béatrice Parfait,[6] Maithé Tauber,[1,2] Jean-Pierre Salles,[1,2] Frank Lezoualc'h,[4] Armelle Yart,[1]* and Patrick Raynal[1,2]*

INSERM U563, Centre de Physiopathologie de Toulouse-Purpan, F-31024 Toulouse, France[1]; CHRU and Université Toulouse III, Hôpital Purpan, F-31059 Toulouse, France[2]; Centre de Biologie du Développement, CNRS UMR5547, F-31062 Toulouse, France[3]; INSERM UMRS 769, Signalisation et Physiopathologie Cardiaque, Université Paris Sud 11, F-92296 Châtenay-Malabry, France[4]; Université Paris Descartes and INSERM U781, Hôpital Necker, F-75743 Paris, France[5]; and Université Paris Descartes and INSERM U745, UFR Pharmacie, F-75270 Paris, France[6]

Received 19 May 2009/Returned for modification 22 December 2009/Accepted 17 February 2010

LEOPARD syndrome (LS), a disorder with multiple developmental abnormalities, is mainly due to mutations that impair the activity of the tyrosine phosphatase SHP2 (*PTPN11*). How these alterations cause the disease remains unknown. We report here that fibroblasts isolated from LS patients displayed stronger epidermal growth factor (EGF)-induced phosphorylation of both AKT and glycogen synthase kinase 3β (GSK-3β) than fibroblasts from control patients. Similar results were obtained in HEK293 cells expressing LS mutants of SHP2. We found that the GAB1/phosphoinositide 3-kinase (PI3K) complex was more abundant in fibroblasts from LS than control subjects and that both AKT and GSK-3β hyperphosphorylation were prevented by reducing GAB1 expression or by overexpressing a GAB1 mutant unable to bind to PI3K. Consistently, purified recombinant LS mutants failed to dephosphorylate GAB1 PI3K-binding sites. These mutants induced PI3K-dependent increase in cell size in a model of chicken embryo cardiac explants and in transcriptional activity of the atrial natriuretic factor (ANF) gene in neonate rat cardiomyocytes. In conclusion, SHP2 mutations causing LS facilitate EGF-induced PI3K/AKT/GSK-3β stimulation through impaired GAB1 dephosphorylation, resulting in deregulation of a novel signaling pathway that could be involved in LS pathology.

Noonan syndrome (NS) (MIM163950) is a relatively frequent (~1/2,000 births) autosomal dominant disease primarily characterized by facial dysmorphism, heart defects, and short stature. LEOPARD syndrome (LS) (MIM151100) is a rarer but related disorder that associates, roughly, NS symptoms with deafness and cutaneous abnormalities. Both NS and LS belong to the family of "neuro-cardio-facial-cutaneous" (NCFC) syndromes, a group of developmental disorders that display different combinations of the above-mentioned symptoms with mental retardation and tumor predisposition (4, 13).

At least 80% of LS and 50% of NS patients carry germ line missense mutations in *PTPN11*, the gene encoding SHP2. SHP2 is a widely expressed protein tyrosine phosphatase (PTP) that contains Src homology 2 (SH2) domains and promotes Ras–mitogen-activated protein kinase (MAPK) activation through different molecular mechanisms (14, 27, 39, 47). Other LS or NS forms are caused by mutations in *KRAS*, *SOS1*, *RAF1*, *BRAF*, and *SHOC2* genes, which encode key factors of the Ras-MAPK pathway (6, 32, 34, 37, 38, 41).

Although genetic studies have provided essential advances, how *PTPN11* mutations cause the diseases' symptoms remains an open question. Biochemical studies have shown that NS mutations are located at contact points between the catalytic and the SH2 domains and therefore disrupt SHP2 autoinhibitory conformation (11, 19), thereby stimulating SHP2 catalytic activity (gain-of-function mutations). Conversely, LS mutations are confined within the catalytic domain and repress SHP2 activity (15, 21, 40).

A key issue in understanding LS/NS pathogenesis is the identification of the signaling pathways that are altered by these mutations. It is now well accepted that NS mutants can exert a dominant-positive effect on Ras-MAPK activation and that this upregulation is responsible for the cardiac defects observed in NS (1, 2, 9, 11, 22, 23, 29). In addition, NS mutations could alter other signaling pathways (Ca^{2+}/NFAT, RhoA, and Src) (17, 42, 44).

In the case of *PTPN11* mutations causing LS, our knowledge is much poorer, since even the outcomes of these mutations for the Ras-MAPK pathway are unclear (21, 31). It is thus important to examine whether these mutations modify other signaling pathways that regulate embryo development. It was shown recently that, besides promoting Ras/MAPK stimulation, wild-type (WT) SHP2 can regulate phosphoinositide 3-kinase (PI3K) activation by growth factors (46). In addition, our recent biochemical study suggests that LS mutations could promote PI3K activation (15). PI3Ks are lipid kinases with major functions during development, as shown by re-

* Corresponding author. Mailing address: INSERM U563, Centre de Physiopathologie de Toulouse-Purpan, BP3028, Toulouse, F-31024, France. Fax: 33-562-748-666. Phone for Patrick Raynal: 33-562-748-671. E-mail: patrick.raynal@inserm.fr. Phone for Armelle Yart: 33-562-748-657. E-mail: armelle.yart@inserm.fr.
† T.E. and J.-P.C. contributed equally to the work.
▽ Published ahead of print on 22 March 2010.

combinant mouse models and human familial diseases. Similarly to Ras/MAPK, PI3K activity is highly regulated by growth factors and is critical for their actions in cell growth, apoptosis, migration, and differentiation (10, 18).

Therefore, we assessed whether LS mutations could influence PI3K activation. To this end, we generated primary and immortalized fibroblast cell lines from LS patients and healthy controls and showed that, in response to epidermal growth factor (EGF) stimulation, PI3K/AKT was upregulated in LS cells. This deregulation was due to impaired dephosphorylation of GAB1 PI3K-binding sites by LS mutants. Furthermore, LS mutants promoted PI3K-dependent upregulation of hypertrophy genes in cardiomyocytes.

MATERIALS AND METHODS

Generation, culture, and stimulation of LS, NS, and control fibroblasts. Primary fibroblast cultures were established from skin biopsy specimens obtained from four different patients (two LS patients carrying the Y279C or T468M mutation and two NS patients with the E76D or N308D mutation) and from two healthy subjects following standard protocols (5) approved by our institutional review board and after informed consent. The fibroblasts were expanded, immortalized with simian virus 40 (SV40), and maintained in Dulbecco's modified Eagle's medium (DMEM) containing 10% fetal bovine serum (FBS) and antibiotics (Invitrogen). Before stimulation, the cells were incubated overnight in serum-free medium. The stimulations were performed using 50 ng/ml EGF (Peprotech) for the indicated times. When indicated, cells were treated, before stimulation, with 20 μM LY294002 or 100 nM wortmannin.

siRNA transfection. Forty-percent-confluent 6-well plates of immortalized fibroblasts were treated with a transfection mixture containing 800 μl DMEM and 200 μl Opti-MEM (Invitrogen) containing GAB1 or control small interfering RNA (siRNA) (Qiagen; catalog no. SI02654736 and 1027310; 30 nM) and 3 μl Oligofectamine (Invitrogen). The cells were incubated in the transfection mixture for 4 h, and then 500 μl DMEM, supplemented with 30% serum and antibiotics, was added to each plate. The cells were again incubated for 24 h and then serum starved overnight and stimulated or not with EGF as indicated.

Western blot analysis. Cells were scraped off in lysis buffer containing 25 mM Tris, pH 7.4, 50 mM KCl, 0.5 mM EDTA, 5% glycerol, 0.5% Triton X-100, 20 mM NaF, 2 mM Na_3VO_4, and protease inhibitors. The cell lysates were cleared by centrifugation, and total proteins were measured using the method of Bradford (Bio-Rad). Lysate aliquots containing identical amounts of proteins were diluted in Laemmli's sample buffer, boiled, and processed for immunoblotting using a standard procedure (7, 36). The polyclonal antibodies used were anti-phospho-AKT-Ser473 and anti-phospho-glycogen synthase kinase 3α/β (GSK-3α/β)-Ser21/9 (Cell Signaling Technology); anti-GAB1, -SHP2, -EGF receptor (EGFR), and -AKT (Santa Cruz); and anti-p85 (Upstate). The monoclonal antibodies were anti-GSK-3β (Cell Signaling), antitubulin (Sigma), antihemagglutinin (anti-HA) (Roche), anti-Myc (Santa Cruz), and anti-V5 (Invitrogen). Horseradish peroxidase (HRP)-conjugated secondary antibodies were from Sigma. Blots were revealed using the Enhanced Chemiluminescence detection system (Amersham).

Transfection of HEK293 cells. Subconfluent HEK293 cells grown in 100-mm plates with DMEM containing 10% FBS and antibiotics (Invitrogen) were transiently transfected with a mixture containing 6 μl of FuGene6 reagent (Roche) and 2 μg of total DNA, according to the manufacturer's instructions. The pcDNA plasmids encoding WT SHP2 and mutants, GAB1-Myc, and HA-AKT were described previously (15, 27, 36) or were obtained using the QuikChange kit (Stratagene). After 24 h, the cells were serum deprived and stimulated as for human fibroblasts.

Immunoprecipitations and GST-p85 pull-downs. Cells were scraped off in lysis buffer containing 20 mM Tris, pH 7.4, 150 mM NaCl, 10 mM EDTA, 10% glycerol, 1% Nonidet P-40, 1 mM Na_3VO_4, and protease inhibitors and then centrifuged to eliminate the insoluble material. For immunoprecipitation, the lysates were incubated with the indicated primary antibodies for 1 h at 4°C, followed by incubation with protein A-Sepharose (Amersham) for 1 h, and then collected by centrifugation and washed with lysis buffer containing 0.1% Nonidet P-40 and 0.1 mM Na_3VO_4. The immunoprecipitates were then processed for Western blot analysis as described above.

The glutathione *S*-transferase (GST) fusion protein containing the SH2 domains of p85 was described previously (7). The fusion protein was expressed in *Escherichia coli* and extracted using glutathione-Sepharose beads (Sigma) in a standard procedure. For GST pull-down experiments, cells were scraped off in 1 ml lysis buffer containing 50 mM Tris, pH 8.0, 150 mM NaCl, 10 mM $MgCl_2$, 0.5% sodium desoxycholate, 1% Nonidet P-40, 0.1% SDS, 1 mM phenylmethylsulfonyl fluoride (PMSF), and 1 μg/ml each of aprotinin and leupeptin. The cleared lysates were incubated at 4°C for 2 h with 3 μg of GST-p85 bound to glutathione-Sepharose beads. The beads were washed three times in lysis buffer and then boiled in electrophoresis sample buffer and processed for Western blotting.

Recombinant proteins and PTP assay. SHP2 mutant cDNAs were subcloned into the pProEX-HT vector to produce recombinant proteins according to the manufacturer's protocol (Invitrogen). Briefly, recombinant proteins were extracted from *E. coli* lysates using Probond resin, and then the beads were washed with buffer containing 20 mM Tris, pH 7.4, 200 mM NaCl, 40 mM imidazole, 1 mM PMSF, and protease inhibitors. Proteins were eluted with 200 mM imidazole. Purification was monitored by SDS-PAGE and Coomassie blue staining. The purified proteins were stored in 33% glycerol at −80°C. PTP assays were performed by incubating 50 ng of each SHP2 recombinant protein in PTP buffer (20 mM HEPES, pH 7.4, 1 mM EDTA, 5% glycerol. 1 mM dithiothreitol [DTT]) with 250 μM substrate phosphopeptide, Src-pY530 (TSTEPQ-pY-QPGENL) or GAB1-pY589 (DSEEN-pY-VPMNPNL), in the presence or absence of activating peptides (IRS1-pY1172, SLN-pY-IDLDLVK) (where pY is phosphotyrosine). After a 30-min incubation at 37°C, the amount of released phosphate was assayed using Malachite Green solution (Upstate Biotechnology). The phosphopeptides were synthesized by NeoMPS.

Generation of recombinant adenoviruses. Bicistronic adenoviruses encoding green fluorescent protein (GFP) and SHP2-WT, -E76D, -N308D, -Y279C, or -T468M were obtained by subcloning the corresponding V5-tagged SHP2 construct into the pTrack-CMV vector. Recombinant adenoviruses were then obtained according to the pAdEasy homologous-recombination system, followed by plaque purification, expansion, and titration in HEK293 cells (16).

Serum response factor (SRF)/myocardin assays with the luciferase reporter gene. Patient fibroblasts (50,000 cells/well) were seeded in 24-well plates 16 h prior to transfection. The transfection mixture contained 1.2 μl of FuGene6 reagent (Roche), 15 ng of serum response element-luciferase reporter gene construct (30), 3 ng of pSV-Renilla luciferase expression vector as an internal control (Promega), 150 ng of myocardin expression vector (43) (unless otherwise indicated), and 160 ng of pcDNA3 plasmid. These optimal concentrations were the result of several experimental trials. The cells were washed in phosphate-buffered saline (PBS) 16 h after transfection and maintained in serum-free DMEM for 24 h. After EGF stimulation, cell extracts were prepared and luciferase activity was determined using the Dual Luciferase kit (Promega). Measurements were made using a Berthold Lumat LB950.

Chicken embryo myocardial explants and fluorescence-activated cell sorter (FACS) analysis. All procedures were approved by the Institutional Animal Care and Use Committee. Fertile hen's eggs obtained from a local supplier were incubated at 38°C to yield embryos at the Hamburger-Hamilton stage 22 (embryonic day 3.5 [E3.5]). Myocardial cushions were excised from embryos, randomly assigned to the different treatment groups, and cultured for 3 days as follows. The cushions were incubated in 50 μl of medium with 10^8 PFU of adenoviruses encoding WT SHP2 or mutants for 30 min before being plated for organotypic cultures (25) in M199 (Cellgro) with 10% FBS (Invitrogen), 1% chicken embryo extract (Sera Laboratories International), and 1% penicillin/streptomycin (Invitrogen). After 24 h, the cushions were incubated in M199 containing 2% FBS for 24 h and finally stimulated with 50 ng/ml EGF for the last 24 h. The myocardial explants were checked for GFP expression to assess the efficiency of adenoviral infection. Images of whole cushions were acquired with an SP2 Leica confocal microscope. At the end of the experiment, the explants were dissociated with trypsin and gentle pipetting. Individual cells were fixed on ice for 15 min with 2% paraformaldehyde, and cell size was analyzed using a FACScan apparatus.

Measurement of ANF transcriptional activity. For measurement of atrial natriuretic factor (ANF) transcriptional activity, neonatal rat ventricular myocytes were isolated as described previously (45) and cultivated in 12-well plates. They were transfected with 0.35 μg DNA of the SHP2 mutant construct and 0.15 μg of plasmid carrying the rat ANF promoter fused to the luciferase reporter gene (ANF-Luc). DNA was mixed with Lipofectamine 2000 (Invitrogen) in Opti-MEM (Invitrogen) according to the manufacturer's instructions and as previously described (26, 28).

Statistics. Results are expressed as means ± standard errors of the mean (SEM) and were compared using a paired Student's *t* test. The number of independent experiments (*n*) is indicated. A *P* value below 0.05 was considered significant.

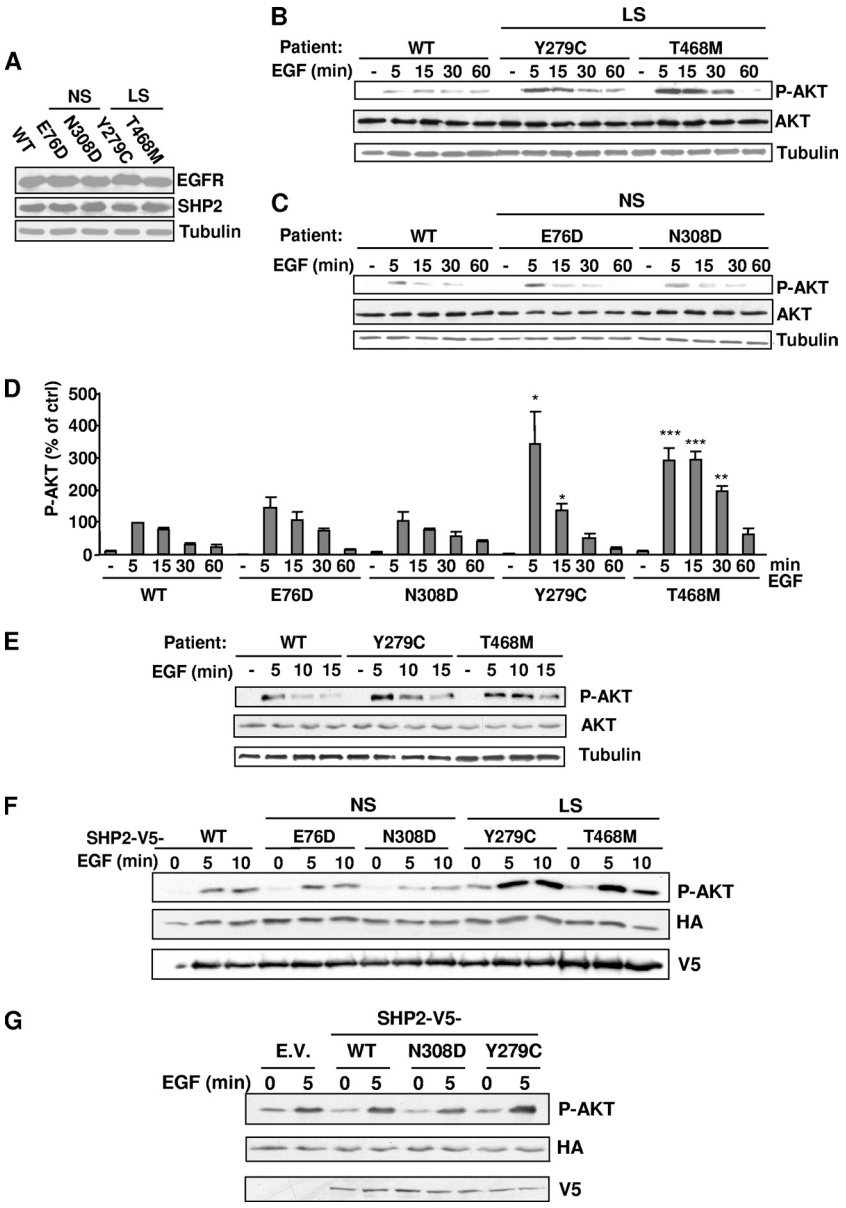

FIG. 1. Dominant-positive activity of LS mutants on AKT phosphorylation. (A) Immortalized skin fibroblasts from healthy subjects (WT) or from LS or NS patients carrying the indicated *PTPN11* mutations were lysed and probed by Western blot analysis to assess the level of EGFR and SHP2 expression. (B and C) The same cells were stimulated with EGF for the indicated times and probed by Western blot analysis to determine the level of AKT phosphorylation with an anti-phospho-AKT (P-AKT) antibody. AKT and tubulin were used as controls for gel loading. (D) P-AKT immunoblots from 3 independent experiments shown in panels B and C were quantified using ImageJ software. Only significant differences versus WT cells for the corresponding time are indicated (*, $P < 0.05$; **, $P < 0.01$; ***, $P < 0.001$; $n = 3$). The error bars indicate SEM. (E) The same experiment as shown in panel B performed with WT and LS fibroblasts prior to immortalization. (F) HEK293 cells were cotransfected with HA-tagged AKT and the indicated V5-tagged SHP2 constructs. Following EGF stimulation, the cells were immunoprecipitated with an anti-HA antibody and then probed with anti-P-AKT or anti-HA antibodies (top and middle gels). Aliquots of corresponding cell lysates were probed with an anti-V5 antibody (bottom gel). (G) The same experiment as shown in panel F performed with the indicated constructs (E. V., empty vector).

RESULTS

Dominant-positive activity of LS *PTPN11* mutants on AKT activation. To explore the possible effects of *PTPN11* mutations on the PI3K/AKT pathway, we monitored AKT phosphorylation following stimulation with EGF in immortalized fibroblasts from LS and NS patients and healthy controls. For this purpose, we measured AKT phosphorylation on Ser-473, which is dependent on PI3K under EGF stimulation (data not shown). The different cell lines express EGFR and SHP2 to similar extents (Fig. 1A), implying that comparison of EGF-stimulated signaling between them could reveal possible effects of the corresponding SHP2 mutation. EGF-induced AKT phosphorylation was significantly more robust in fibroblasts from the two LS patients (Y279C and T468M) (Fig. 1B) than in NS cells (E76D and N308D) (Fig. 1C) compared to healthy controls (Fig. 1D). To ensure that immortalization did

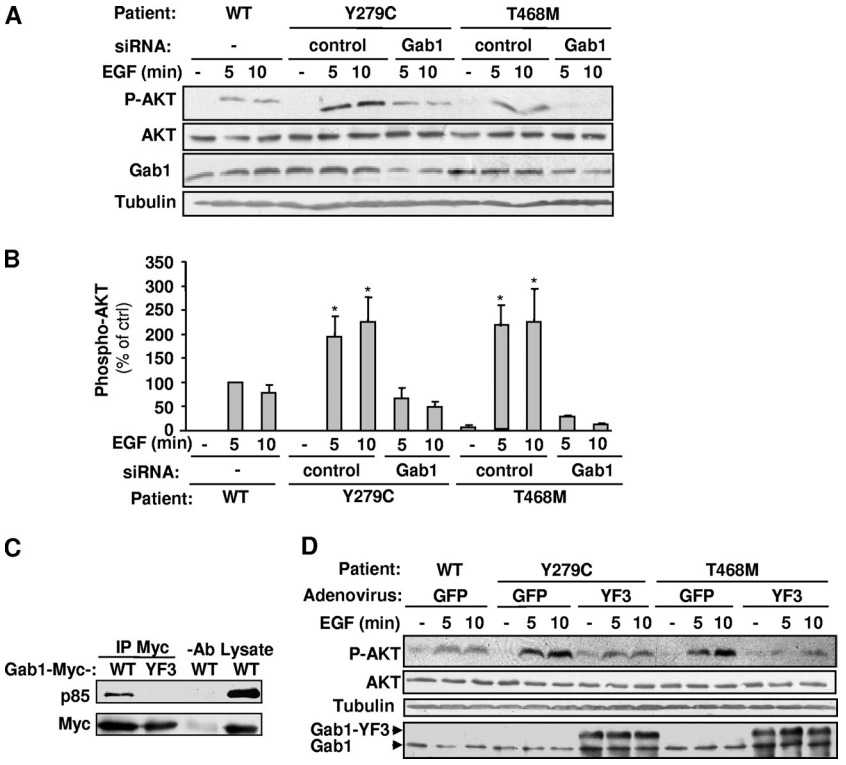

FIG. 2. LS mutant-induced PI3K upregulation is dependent on GAB1-mediated PI3K recruitment. (A) Immortalized skin fibroblasts from a healthy subject (WT) or from LS patients carrying the indicated *PTPN11* mutations were transfected with control or GAB1 siRNA, as indicated, before stimulation with EGF for the indicated times. The cells were then processed for Western blot analysis and probed with the indicated antibodies. (B) Immunoblots performed for panel A were quantified using ImageJ. Only significant differences versus WT cells for the corresponding time are indicated (*, $P < 0.05$; $n = 3$). The error bars indicate SEM. (C) HEK293 cells were transfected with constructs encoding Myc-tagged GAB1-WT or GAB1-YF3. Following EGF stimulation, the cells were subjected to anti-Myc immunoprecipitation (IP) and then analyzed by anti-p85 (top) or anti-Myc (bottom) immunoblotting. −Ab WT, mock immunoprecipitation performed from GAB1-WT-transfected cells without primary antibody; Lysate WT, aliquot of transfected cell lysate loaded on the gel as a positive control for Western blot revelation. (D) WT or LS fibroblasts were infected with adenoviruses encoding GAB1-YF3 or GFP as a control, as shown. Following stimulation with EGF, the cells were processed for Western blot analysis and probed with the indicated antibodies.

not influence AKT phosphorylation, the same experiment was also performed in LS and control fibroblasts before immortalization, with results comparable to those obtained with immortalized cells (Fig. 1E).

To further confirm this effect of LS mutations on the PI3K/AKT pathway, we monitored AKT phosphorylation in HEK293 cells, a standard model for the analysis of SHP2 molecular functions (21, 36), transfected with the corresponding LS and NS mutants, together with HA-AKT. SHP2-Y279C and -T468M mutants reinforced EGF-induced AKT phosphorylation in comparison to WT SHP2 and the NS mutants (E76D and N308D) (Fig. 1F). Similar results were obtained with other LS (Q510P) or NS (D61del and E139D) mutants (data not shown). As a control, we verified that expression of WT SHP2 did not significantly modify AKT phosphorylation compared to cells transfected with an empty vector (Fig. 1G).

These results indicate that SHP2 mutants identified in LS patients have a dominant-positive effect on AKT activation.

LS mutants promote PI3K/AKT upregulation through impaired dephosphorylation of GAB1 PI3K-binding sites. We next investigated how LS mutants exerted a dominant-positive effect on PI3K/AKT activation. EGF-dependent PI3K/AKT stimulation relies on GAB1, a docking protein phosphorylated by EGF receptor on specific tyrosine residues involved in PI3K recruitment via its p85 regulatory unit (24). Since SHP2 can dephosphorylate these PI3K-binding sites to regulate PI3K/AKT activation (46), we hypothesized that a defect in this regulatory activity in LS patients could lead to increased EGF-induced PI3K activation, which would explain the stronger AKT activation observed in LS fibroblasts.

To test this hypothesis, we determined whether siRNA-mediated suppression of GAB1 expression had an effect on AKT hyperphosphorylation in LS cells. Upon reduction of GAB1 expression, AKT hyperphosphorylation was decreased (Fig. 2A), and a quantitative analysis showed a similar effect of GAB1 siRNA in decreasing AKT phosphorylation in fibroblasts obtained from both LS patients (Fig. 2B). This suggested that GAB1 was involved in PI3K/AKT upregulation in LS cells. To further validate this hypothesis, we analyzed EGF-induced AKT phosphorylation in LS cells transfected with the GAB1-YF3 mutant. This construct is mutated on its three PI3K-binding sites, and we verified that it is unable to associate with PI3K (p85) (Fig. 2C). When overexpressed in LS patient cells, GAB1-YF3 reduced AKT hyperphosphorylation, whereas, as a control, GFP had no effect (Fig. 2D). Hence, this result supported the above hypothesis.

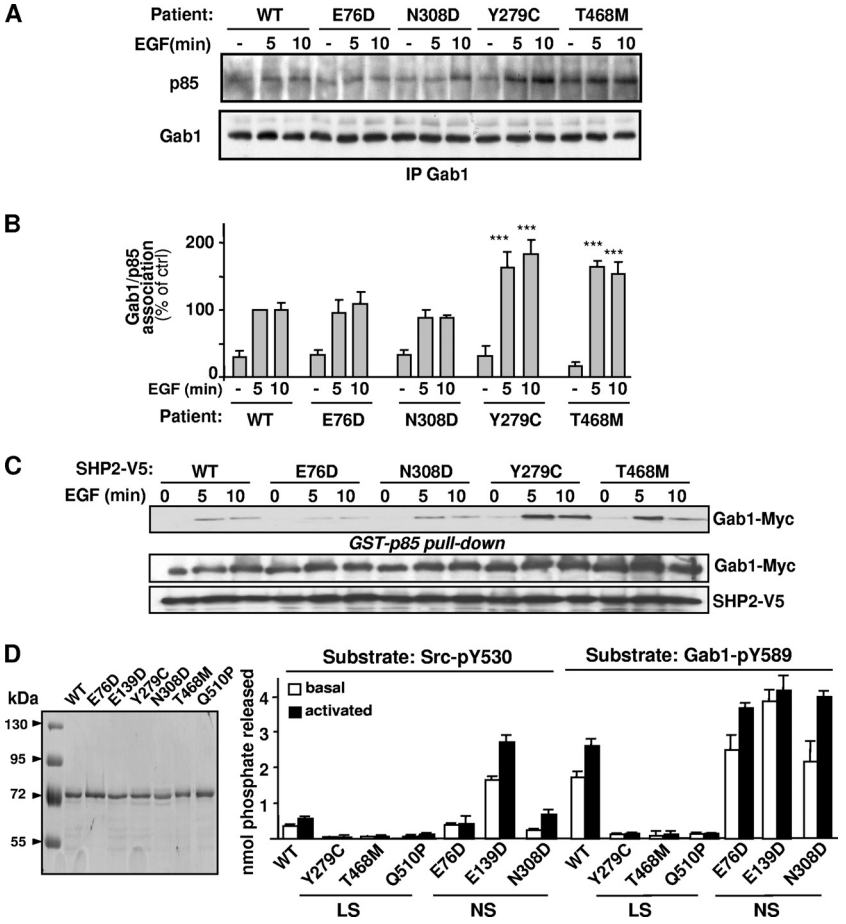

FIG. 3. LS mutants impair dephosphorylation of GAB1 PI3K-binding sites. (A) WT, NS, or LS fibroblasts were stimulated with EGF for the indicated times and then immunoprecipitated with an anti-GAB1 antibody and probed for p85 and GAB1. (B) Quantification of p85 precipitation using ImageJ. Only significant differences versus WT cells for the corresponding time are indicated (***, $P < 0.001$; $n = 3$). The error bars indicate SEM. (C) HEK293 cells were transfected with Myc-tagged GAB1 and the indicated V5-SHP2 constructs and then subjected to a PI3K affinity precipitation assay (pull-down) using a GST-PI3K (GST-p85) fusion protein. The amount of precipitated GAB1-Myc was analyzed with an anti-Myc antibody (top gel). Aliquots of corresponding lysates were probed with anti-Myc and anti-V5 antibodies (middle and bottom gels). (D) Analysis of recombinant LS and NS SHP2 mutants by *in vitro* phosphatase assays. (Left) Two micrograms of the indicated recombinant SHP2 proteins was analyzed by SDS-PAGE and Coomassie blue staining. (Right) Phosphatase assays were performed by incubating the indicated recombinant SHP2 proteins with Src-pY530 or GAB1-pY589 phosphopeptide as a phosphatase substrate. The assays were performed in the presence or absence of an SHP2-activating peptide, as indicated.

To assess whether this PI3K/AKT upregulation was due to increased interaction between GAB1 and PI3K, we measured the GAB1/PI3K association in WT, NS, and LS cells by coimmunoprecipitating GAB1 with p85 following stimulation with EGF. The amount of p85 that was present in GAB1 immunoprecipitates was significantly higher in LS cells than in control or NS cells (Fig. 3A and B). This suggests that LS mutations favor sustained binding of GAB1 to PI3K, which may explain why in LS cells AKT is hyperphosphorylated.

To further examine whether LS mutations promoted GAB1/PI3K binding through impaired dephosphorylation of GAB1, we analyzed GAB1 phosphorylation on its PI3K-binding sites in HEK293 cells transfected with the LS (SHP2-Y279C and -T468M) and NS (SHP2-E76D and -N308D) mutants. For convenience, we affinity precipitated GAB1 with a GST-p85 fusion protein, which allowed us to precipitate GAB1 when phosphorylated on its PI3K-binding sites (7). Figure 3C shows that, in comparison with WT SHP2, the LS mutants, but not the NS mutants, facilitated GST-p85/GAB1 association, implying sustained phosphorylation of GAB1 on its PI3K-binding sites. This reinforced the hypothesis that LS mutants promote PI3K/AKT activation by facilitating PI3K recruitment by GAB1.

To further assess the impact of LS mutants on GAB1/PI3K interaction, we measured *in vitro* the catalytic activity of LS mutants on a synthetic phosphopeptide carrying one of GAB1 PI3K-binding sites (GAB1-pY589). To this end, we produced LS (Y279C, T468M, and Q510P) and NS (E76D, E139D, and N308D) mutants as purified recombinant proteins (Fig. 3D, left) to be used for *in vitro* PTP assays. The results (Fig. 3D, right) confirmed previous observations that LS mutants display extremely low enzymatic activity (15, 21, 40) when assayed using a standard PTP substrate (Src-pY530). In addition, similar results were obtained using a more specific SHP2 substrate (GAB1-pY589), suggesting that all LS mutants have similar biochemical features.

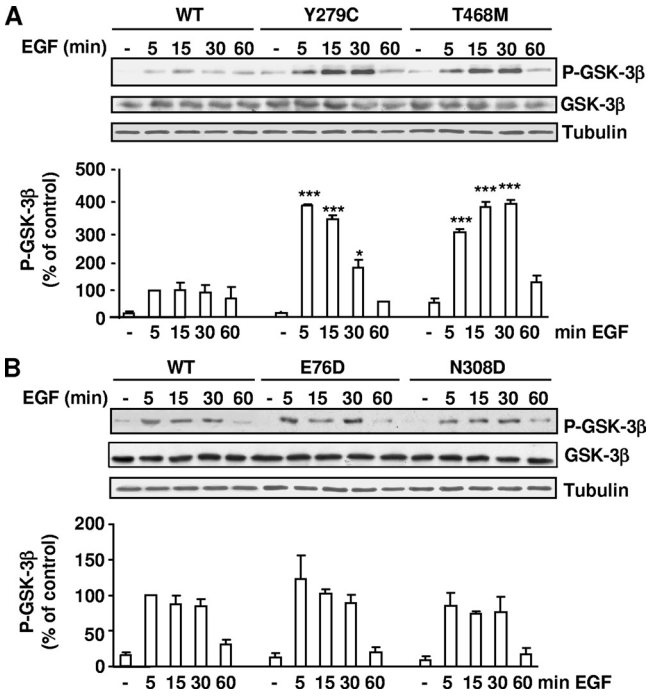

FIG. 4. LS fibroblasts display enhanced EGF-induced GSK-3β phosphorylation. (A) (Top) Immortalized WT and LS (T468M or Y279C mutation) fibroblasts were stimulated with EGF and then processed for Western blot analysis and probed with anti-phospho-GSK-3β (P-GSK-3β), anti-total GSK-3β, and antitubulin antibodies. (Bottom) P-GSK-3β immunoblots were quantified using ImageJ. Only significant differences versus WT cells for the corresponding time are indicated (*, $P < 0.05$; ***, $P < 0.001$; $n = 3$). The error bars indicate SEM. (B) The same experiment as shown in panel A with cells from WT or NS patients carrying the indicated *PTPN11* mutations.

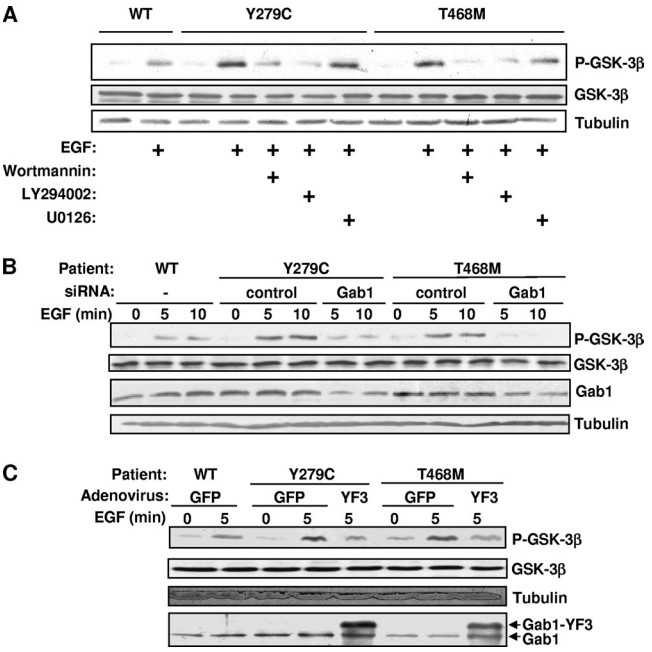

FIG. 5. LS mutants promote EGF-induced GSK-3β phosphorylation through a PI3K- and GAB1-dependent pathway. (A) Immortalized skin fibroblasts from a healthy subject (WT) or LS patients carrying the indicated *PTPN11* mutations were treated or not with the indicated inhibitors for 30 min before stimulation with EGF, as shown. The cells were then lysed and processed for anti-P-GSK-3β and antitubulin immunoblotting. (B) WT and LS fibroblasts were transfected with control or GAB1 siRNA, as indicated, before stimulation with EGF. The cells were then processed for Western blot analysis and probed with the indicated antibodies. (C) WT and LS cells were infected with adenoviruses encoding GAB1-YF3 or GFP as a control, as shown. Following stimulation with EGF, the cells were processed for Western blot analysis and probed with the indicated antibodies.

Taken together, these results demonstrate that LS mutants promote GAB1/PI3K association as a consequence of impaired dephosphorylation of GAB1 PI3K-binding sites by these mutants. This explains why LS mutants exert a dominant-positive effect on EGF-induced PI3K/AKT activation.

LS mutants promote GSK-3β phosphorylation in LS cells through a PI3K-dependent pathway. We then investigated which signaling pathways downstream of PI3K/AKT could be deregulated in LS. A good candidate was GSK-3β, a multifunctional kinase involved in embryo development (12). To determine whether GSK-3β was deregulated in LS, we measured GSK-3β phosphorylation on Ser-9, a key regulatory residue which, when phosphorylated by AKT, represses GSK-3β activity. EGF-induced GSK-3β phosphorylation was significantly higher in LS fibroblasts than in control and NS cells (Fig. 4A and B). We then verified whether GSK-3β hyperphosphorylation in LS cells was linked to PI3K/AKT upregulation. For this purpose, we treated LS cells with standard PI3K pharmacological inhibitors (LY294002 and wortmannin) before probing for GSK-3β phosphorylation. As shown in Fig. 5A, this treatment virtually abolished the EGF-induced GSK-3β hyperphosphorylation, while the Ras-MAPK inhibitor U0126 had only a minor effect. This result indicates that GSK-3β hyperphosphorylation in LS is PI3K dependent, suggesting that GSK-3β deregulation in LS could be a consequence of PI3K/AKT upregulation.

To further test this hypothesis, we examined whether GAB1 was also implicated in GSK-3β deregulation. Reduction of GAB1 expression by siRNA in LS fibroblasts suppressed GSK-3β hyperphosphorylation (Fig. 5B). To further assess GAB1 involvement, we monitored GSK-3β phosphorylation in LS cells infected with GAB1-YF3 adenoviruses. GAB1-YF3, but not GFP, overexpression resulted in the suppression of GSK-3β hyperphosphorylation (Fig. 5C). Thus, disruption of GAB1 PI3K-binding sites prevents GSK-3β hyperphosphorylation in LS cells, supporting the hypothesis that GSK-3β deregulation is the result of GAB1-mediated PI3K/AKT upregulation.

LS mutant-dependent PI3K hyperactivation enhances myocardin/SRF activity. Previous reports had shown that GSK-3β, among different targets, regulates myocardin, a transcriptional cofactor of the SRF (3, 20, 43). Therefore, we wondered whether LS-induced PI3K/GSK-3β deregulation could affect myocardin activity. As a first attempt to test this hypothesis, we assessed whether LS or NS mutants of SHP2 could modulate myocardin activity. To this end, WT, LS, and NS fibroblasts were transfected with increasing amounts of myocardin before SRF activity was monitored. As shown in Fig. 6A, myocardin expression in patient fibroblasts induced a dose-response in-

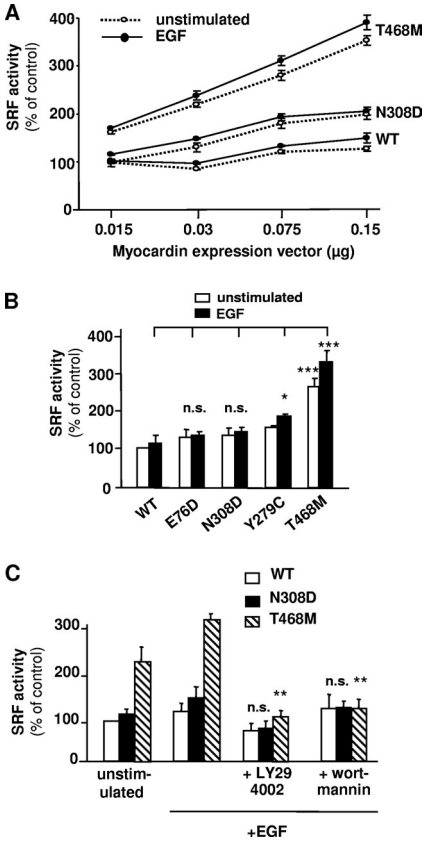

FIG. 6. LS mutations promote upregulation of SRF activity through a PI3K-dependent pathway. (A) SRF activity was measured using a luciferase gene reporter assay in LS (T468M), NS (N308D), and control (WT) fibroblasts in the presence of increasing concentrations of myocardin. The error bars indicate SEM. (B) The same experiment as shown in panel A performed with all available patient cell lines. Significant differences versus stimulated WT cells are indicated (*, $P < 0.05$; ***, $P < 0.001$; n.s., not significant). (C) The same experiment as shown in panel A performed in the presence of the indicated inhibitors. **, $P < 0.01$; n.s., not significant. Significant differences versus corresponding cells, stimulated with EGF in the absence of inhibitor, are indicated.

crease in SRF activity. Interestingly, we observed a stronger response in T468M LS cells than in WT or N308D NS cells (Fig. 6A). We next compared SRF activities in fibroblasts from all available patients and confirmed that EGF-induced SRF activity was significantly higher in the two LS cell lines than in cells from NS patients or healthy controls (Fig. 6B). Of note, SRF activity in the unstimulated and EGF-stimulated states was higher in the LS cells, particularly the T468M mutant. The fact that SRF deregulation appeared stronger in T468M than in Y279C fibroblasts is probably a consequence of a more robust AKT deregulation in T468M than in Y279C fibroblasts (Fig. 1B). We then assessed whether the increased SRF/myocardin activity in LS fibroblasts was mediated by PI3K upregulation. PI3K inhibition by LY294002 or wortmannin abolished the myocardin-dependent SRF stimulation observed in the T468M LS cell line (Fig. 6C). Consequently, these data suggest that LS-induced PI3K upregulation can enhance SRF/myocardin activity in a reconstituted model.

LS mutant-induced PI3K upregulation promotes hypertrophic growth in chicken embryo explants and ANF expression in cultured cardiomyocytes. Since GSK-3β activity/activation and subsequent inhibition of myocardin-dependent transcriptional transactivating activity may be involved in reduced cardiomyocyte hypertrophy (3), we hypothesized that LS mutants could promote hypertrophy in a PI3K-dependent manner. In human primary cells derived from adult heart ventricles, we observed that LS, but not NS, mutants induced AKT and GSK-3β hyperphosphorylation (data not shown), suggesting that LS mutants can cause deregulation of the PI3K/AKT/GSK-3β pathway in cardiac cells. Next, we analyzed the effect of LS mutations on the size of primary cells derived from chicken embryo myocardial cushions following adenoviral infection of the most "signal-altering" LS mutant (SHP2-T468M) in the tissue. After stimulation with EGF, explants were dissociated, and the sizes of individual cells were assessed by FACS analysis. Interestingly, the size of cells expressing the LS mutant SHP2-T468M was increased in comparison with cells infected with WT SHP2. Moreover, following PI3K inhibition with LY294002 (LY), the most stable and the least toxic of the two PI3K inhibitors, the shift of cell size induced by the LS mutant was abolished (Fig. 7A). Of note, under those experimental settings, the size of noninfected, GFP-negative cells was not significantly modified by LY294002 treatment (data not shown). This signifies that the cell size enlargement in tissue infected with the LS mutant was dependent on PI3K.

Finally, we evaluated whether LS-induced deregulation of the PI3K/AKT/GSK-3β pathway was associated with cardiomyocyte hypertrophy. Reexpression of embryonic genes, including ANF, and transient activation of immediate-early genes are frequently used as markers of myocyte hypertrophy. Therefore, to test whether LS mutants could induce cardiomyocyte hypertrophy, we overexpressed SHP2-WT, N308D, or T468M in neonatal rat ventricular myocytes, and we studied their impacts on ANF expression using a luciferase gene reporter assay. SHP2-T468M induced a stronger ANF-luciferase response than WT SHP2 or the NS mutant SHP2-N308D (Fig. 7B). This higher ANF transcriptional activity was abolished by LY294002, suggesting that LS mutants could promote cardiomyocyte hypertrophy through PI3K upregulation.

DISCUSSION

In this study, we analyzed the effect of SHP2 mutations identified in LS patients on the PI3K/AKT pathway. Upon EGF induction, AKT was hyperphosphorylated both in LS fibroblasts and in HEK293 cells overexpressing the corresponding LS mutants. We then analyzed in detail the mechanism of PI3K/AKT upregulation by LS mutants and obtained the following data: (i) reducing GAB1 expression using siRNA prevents PI3K/AKT upregulation in LS patient cells, (ii) adenovirus-driven expression of GAB1-YF3 (deficient for PI3K binding) suppresses AKT upregulation in LS cells, (iii) the amount of GAB1/PI3K complex is higher in LS cells than in cells from healthy subjects or NS cells, and (iv) recombinant LS SHP2 mutants are particularly inactive in dephosphorylating a peptide carrying a GAB1 PI3K-binding site, whereas WT SHP2 or NS mutants dephosphorylate this peptide more efficiently than a standard PTP substrate. All these observations

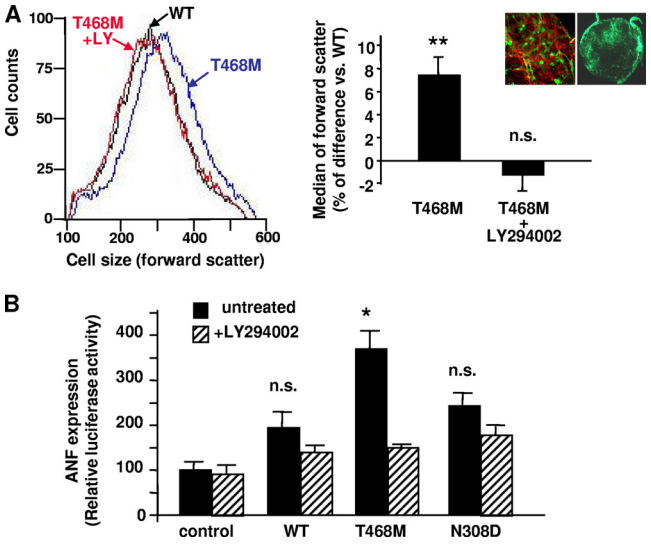

FIG. 7. An LS mutant enhances ANF expression and promotes cardiac cell hypertrophy through a PI3K-dependent pathway. (A) Myocardial cushions from chicken embryos were infected with adenoviruses expressing GFP and a SHP2-WT, or -T468M mutant. After stimulation with EGF, the sizes of cushion cells were measured by FACS. (Left) FACS profile from a representative experiment. (Right) Medians of FACS profiles from 3 different experiments. The error bars indicate SEM. (Inset) Confocal images of GFP and rhodamin-phalloidin staining showing tissue integrity at the end of the experiment (left) and GFP staining of a whole cushion infected with SHP2-WT adenoviruses (right). (B) Neonatal rat cardiomyocytes were cotransfected with the indicated SHP2 construct (WT, N308D, or T468M) and a luciferase (Luc) construct under the control of the ANF promoter. Two days after transfection, the cells were assayed for Luc activity. When indicated, the cells were treated, before the Luc assay, overnight with LY294002 (control, cotransfection of ANF-Luc and empty vector). The graphs are presented as the mean and SEM of 3 independent experiments performed in duplicate. In panel A, significant differences versus stimulated WT cells are indicated. In panel B, significant differences versus the untreated control are indicated. (*, $P < 0.05$; **, $P < 0.01$; n.s., not significant.)

indicate that LS mutants cannot efficiently dephosphorylate GAB1 PI3K-binding sites. This defect in SHP2 catalytic activity leads to the upregulation of PI3K/AKT observed in LS cells.

The fact that SHP2-LS mutants have a stimulatory effect on PI3K/AKT in transfected cells and patient fibroblasts is probably the consequence of a dominant-positive effect of these mutants on EGF-induced PI3K/AKT stimulation. In transfected cells, this is certainly due to the recruitment into signaling complexes of transfected SHP2 mutants in lieu of endogenous WT SHP2. Indeed, those mutants possess all the functional domains to be recruited in signaling complexes (SH2 domains and phosphorylation sites). Therefore, it is likely that the mutants compete with endogenous SHP2 for SHP2-binding sites, and since they are overexpressed by transfection, they substitute for endogenous SHP2. As they carry a point mutation that alters their catalytic activity, they cannot complement endogenous SHP2 function, i.e., downregulation of EGF-induced AKT activation. Thus, substitution of endogenous SHP2 by inactive LS mutants in signaling complexes results in AKT upregulation.

In the case of patient cells, SHP2 produced from the mutated allele is not overexpressed compared to SHP2 produced from the WT allele, and the two forms of protein are probably equimolar. Therefore, while in healthy subjects signaling complexes contain 100% WT SHP2, in patient cells, the signaling complexes are composed of 50% WT SHP2 and 50% mutated SHP2. In the case of LS mutants, this is apparently enough to alter SHP2-dependent AKT activation. Of note, in the case of NS patients, others have concluded that NS mutations exert a dominant-positive effect on Ras/MAPK activation through a similar mechanism, considering that WT SHP2 promotes Ras/MAPK activation and that catalytically hyperactive SHP2 NS mutants seem to hyperactivate Ras/MAPK (2, 11).

In a former study, one (T468M) out of three tested LS mutants appeared somewhat able to dephosphorylate a GAB1 phosphopeptide in an vitro assay, even though this mutant, like the others, was deficient in its catalytic activity on a standard phosphatase substrate (15). To clarify this point, in the current work, we produced LS mutants as purified recombinant proteins. This allowed us to perform a study of these mutants' catalytic activities that was more thorough and reliable than what has been achieved thus far. The results (Fig. 3D) showed that the three LS mutants were equally defective in dephosphorylating GAB1, which does not confirm that the T468M mutant behaves differently from other LS mutants.

In addition, our previous study suggested that the T468M mutant, when overexpressed in Vero cells, retained some phosphatase activity toward the PI3K-binding sites borne by GAB1, whereas the Y279C mutant did not. In contrast, in the current study, when transfected in a more standard cell line for signaling studies (HEK293), the T468M and Y279C mutants behaved similarly. More importantly, both mutants displayed the same dominant-positive effect in patient cells, with the T468M mutant being even stronger than the Y279C mutant. The lack of effect of T468M in Vero cells is likely not due to the level of mutant overexpression, since we could observe the dominant-positive effect of the T468M mutant in patient cells that did not overexpress the mutant. Thus, one may assume that the mutations can have different "biological penetrance" in a given cell type, depending, possibly, on the expression level of the binding partners or on the level of stimulation. Supporting this view is a report showing that an NS-causing SHP2 mutation has differential effects on an intracellular signaling pathway when different cell types carrying the mutation are considered (2).

Different mechanisms can be imagined to explain PI3K/AKT upregulation (increased adapter phosphorylation, Ras-mediated hyperactivation of PI3K, increased ErbB3 phosphorylation, decreased PTEN activity, etc.). In this study, we used siRNA targeting GAB1 as a first approach to determine whether this adapter protein was involved in PI3K/AKT upregulation. The fact that GAB1 siRNA suppressed PI3K/AKT upregulation suggested that GAB1 was involved in the process. Then, we explored in detail the role of GAB1, by using the GAB1-YF3 mutant and by analyzing GAB1/PI3K association. The results of these experiments clearly supported the view that increased PI3K recruitment on GAB1 was an important cause of PI3K/AKT upregulation. However, this does not exclude the possibility that future studies could identify other mechanisms also participating in LS-associated PI3K/AKT deregulation, notably those involving Ras, which is most likely deregulated in LS.

Our study also revealed that the phosphorylation of GSK-3β on Ser-9, a major regulatory site, is enhanced in LS fibroblasts. This is certainly a consequence of PI3K/AKT upregulation in LS cells, as this site is a well-established phosphorylation target of AKT (12). Supporting this view is our observation that in LS cells, Ser-9 phosphorylation showed a requirement for PI3K or GAB1 (Fig. 5). Interestingly, GSK-3β is a multifunctional kinase with key functions during embryo development (12). Consequently, it will be interesting to examine whether GSK-3β deregulation is associated with LS symptoms, and notably hypertrophic cardiomyopathy, considering that cardiomyocyte hypertrophy can involve GSK-3β (20). Nevertheless, deregulated pathways distinct from PI3K/AKT/GSK-3β certainly participate in this cardiopathy, as shown by a recent report involving Raf1 gain-of-function in NS or LS patients with hypertrophic cardiomyopathy (32).

Taking into consideration that catalytically inactive LS mutants promote PI3K/AKT upregulation through impaired GAB1 dephosphorylation, one may wonder why hyperactive NS mutants did not downregulate PI3K/AKT, since they seemed to facilitate GAB1 dephosphorylation. A possible explanation could be linked to the gain-of-function effects of NS mutants on Ras/MAPK (13). Indeed, it is now well established that, at least in the case of oncogenic Ras mutants, activated Ras stimulates PI3K through direct interaction (33). In the case of NS mutants, increased Ras activity should lead to higher-than-normal PI3K activation, which could compensate for the inhibitory effect on PI3K due to GAB1 dephosphorylation. Specific studies will be needed to solve this issue, as PI3K activation is a very dynamic process. Indeed, the possibility that NS mutants alter this signaling pathway under particular conditions not tested in our study cannot be excluded.

In conclusion, this report shows that LS-causing *PTPN11* mutations cause abnormal upregulation of the PI3K/AKT/GSK-3β pathway. In light of these findings, it will be interesting to examine whether this pathway deregulation is involved in the development of LS symptoms. The relevance of this research is reinforced by recent reports suggesting that, in addition to Ras-MAPK signaling defects, PI3K-dependent pathways could be altered in other NCFC syndromes (8, 35).

ACKNOWLEDGMENTS

This work was supported by grants from the Agence Nationale de la Recherche (Programme Maladies Rares), Association pour la Recherche sur le Cancer, Ligue Nationale contre le Cancer (sections Aude, Haute-Garonne, Tarn, and Tarn-et-Garonne), E-Rare (NS-EuroNet), and Fondation pour la Recherche Médicale.

We are grateful to T. Levade for cell line immortalization. We thank E. Olson, R. Hipskind, S. Roche, C. Racaud-Sultan, and B. Mariamé for reagents; E. Agius for valuable assistance in organotypic culture; M. Mus, A. Bros, and N. Malet for valuable technical help; A. Montagner and M. Dance for helpful discussions; and F. L'Faqihi and V. Duplan-Eche for FACS analysis.

REFERENCES

1. **Araki, T., G. Chan, S. Newbigging, L. Morikawa, R. T. Bronson, and B. G. Neel.** 2009. Noonan syndrome cardiac defects are caused by PTPN11 acting in endocardium to enhance endocardial-mesenchymal transformation. Proc. Natl. Acad. Sci. U. S. A. **106:**4736–4741.
2. **Araki, T., M. G. Mohi, F. A. Ismat, R. T. Bronson, I. R. Williams, J. L. Kutok, W. Yang, L. I. Pao, D. G. Gilliland, J. A. Epstein, and B. G. Neel.** 2004. Mouse model of Noonan syndrome reveals cell type- and gene dosage-dependent effects of Ptpn11 mutation. Nat. Med. **10:**849–857.
3. **Badorff, C., F. H. Seeger, A. M. Zeiher, and S. Dimmeler.** 2005. Glycogen synthase kinase 3beta inhibits myocardin-dependent transcription and hypertrophy induction through site-specific phosphorylation. Circ. Res. **97:**645–654.
4. **Bentires-Alj, M., M. I. Kontaridis, and B. G. Neel.** 2006. Stops along the RAS pathway in human genetic disease. Nat. Med. **12:**283–285.
5. **Chatelut, M., K. Harzer, H. Christomanou, J. Feunteun, M. T. Pieraggi, B. C. Paton, Y. Kishimoto, J. S. O'Brien, J. P. Basile, J. C. Thiers, R. Salvayre, and T. Levade.** 1997. Model SV40-transformed fibroblast lines for metabolic studies of human prosaposin and acid ceramidase deficiencies. Clin. Chim. Acta **262:**61–76.
6. **Cordeddu, V., E. Di Schiavi, L. A. Pennacchio, A. Ma'ayan, A. Sarkozy, V. Fodale, S. Cecchetti, A. Cardinale, J. Martin, W. Schackwitz, A. Lipzen, G. Zampino, L. Mazzanti, M. C. Digilio, S. Martinelli, E. Flex, F. Lepri, D. Bartholdi, K. Kutsche, G. B. Ferrero, C. Anichini, A. Selicorni, C. Rossi, R. Tenconi, M. Zenker, D. Merlo, B. Dallapiccola, R. Iyengar, P. Bazzicalupo, B. D. Gelb, and M. Tartaglia.** 2009. Mutation of SHOC2 promotes aberrant protein N-myristoylation and causes Noonan-like syndrome with loose anagen hair. Nat. Genet. **41:**1022–1026.
7. **Dance, M., A. Montagner, A. Yart, B. Masri, Y. Audigier, B. Perret, J. P. Salles, and P. Raynal.** 2006. The adaptor protein GAB1 couples the stimulation of vascular endothelial growth factor-2 to the activation of phosphoinositide 3-kinase. J. Biol. Chem. **281:**23285–23295.
8. **Dasgupta, B., Y. Yi, D. Y. Chen, J. D. Weber, and D. H. Gutmann.** 2005. Proteomic analysis reveals hyperactivation of the mammalian target of rapamycin pathway in neurofibromatosis 1-associated human and mouse brain tumors. Cancer Res. **65:**2755–2760.
9. **Eminaga, S., and A. M. Bennett.** 2008. Noonan syndrome-associated SHP-2/Ptpn11 mutants enhance SIRPalpha and PZR tyrosyl phosphorylation and promote adhesion-mediated ERK activation. J. Biol. Chem. **283:**15328–15338.
10. **Engelman, J. A., J. Luo, and L. C. Cantley.** 2006. The evolution of phosphatidylinositol 3-kinases as regulators of growth and metabolism. Nat. Rev. Genet. **7:**606–619.
11. **Fragale, A., M. Tartaglia, J. Wu, and B. D. Gelb.** 2004. Noonan syndrome-associated SHP2/PTPN11 mutants cause EGF-dependent prolonged GAB1 binding and sustained ERK2/MAPK1 activation. Hum. Mutat. **23:**267–277.
12. **Frame, S., and P. Cohen.** 2001. GSK3 takes centre stage more than 20 years after its discovery. Biochem. J. **359:**1–16.
13. **Gelb, B. D., and M. Tartaglia.** 2006. Noonan syndrome and related disorders: Dysregulated RAS-mitogen activated protein kinase signal transduction. Hum. Mol. Genet. **15**(Spec. 2)**:**R220–R226.
14. **Hanafusa, H., S. Torii, T. Yasunaga, K. Matsumoto, and E. Nishida.** 2004. SHP2, an SH2-containing protein tyrosine phosphatase, positively regulates receptor tyrosine kinase signaling by dephosphorylating and inactivating the inhibitor sprouty. J. Biol. Chem. **279:**22992–22995.
15. **Hanna, N., A. Montagner, W. H. Lee, M. Miteva, M. Vidal, M. Vidaud, B. Parfait, and P. Raynal.** 2006. Reduced phosphatase activity of SHP-2 in LEOPARD syndrome: consequences for PI3K binding on GAB1. FEBS Lett. **580:**2477–2482.
16. **He, T. C., S. Zhou, L. T. da Costa, J. Yu, K. W. Kinzler, and B. Vogelstein.** 1998. A simplified system for generating recombinant adenoviruses. Proc. Natl. Acad. Sci. U. S. A. **95:**2509–2514.
17. **Jopling, C., D. van Geemen, and J. den Hertog.** 2007. SHP2 knockdown and Noonan/LEOPARD mutant SHP2-induced gastrulation defects. PLoS Genet. **3:**e225.
18. **Katso, R., K. Okkenhaug, K. Ahmadi, S. White, J. Timms, and M. D. Waterfield.** 2001. Cellular function of phosphoinositide 3-kinases: implications for development, homeostasis, and cancer. Annu. Rev. Cell Dev. Biol. **17:**615–675.
19. **Keilhack, H., F. S. David, M. McGregor, L. C. Cantley, and B. G. Neel.** 2005. Diverse biochemical properties of SHP2 mutants. Implications for disease phenotypes. J. Biol. Chem. **280:**30984–30993.
20. **Kerkela, R., K. Woulfe, and T. Force.** 2007. Glycogen synthase kinase-3β: Actively inhibiting hypertrophy. Trends Cardiovasc. Med. **17:**91–96.
21. **Kontaridis, M. I., K. D. Swanson, F. S. David, D. Barford, and B. G. Neel.** 2006. PTPN11 (SHP2) mutations in LEOPARD syndrome have dominant negative, not activating, effects. J. Biol. Chem. **281:**6785–6792.
22. **Krenz, M., J. Gulick, H. E. Osinska, M. C. Colbert, J. D. Molkentin, and J. Robbins.** 2008. Role of ERK1/2 signaling in congenital valve malformations in Noonan syndrome. Proc. Natl. Acad. Sci. U. S. A. **105:**18930–18935.
23. **Krenz, M., K. E. Yutzey, and J. Robbins.** 2005. Noonan syndrome mutation Q79R in SHP2 increases proliferation of valve primordial mesenchymal cells via extracellular signal-regulated kinase 1/2 signaling. Circ. Res. **97:**813–820.
24. **Mattoon, D. R., B. Lamothe, I. Lax, and J. Schlessinger.** 2004. The docking protein GAB1 is the primary mediator of EGF-stimulated activation of the PI-3K/AKT cell survival pathway. BMC Biol. **2:**24.
25. **Mekki-Dauriac, S., E. Agius, P. Kan, and P. Cochard.** 2002. Bone morphogenetic proteins negatively control oligodendrocyte precursor specification in the chick spinal cord. Development **129:**5117–5130.
26. **Metrich, M., A. Lucas, M. Gastineau, J. L. Samuel, C. Heymes, E. Morel, and F. Lezoualc'h.** 2008. Epac mediates beta-adrenergic receptor-induced cardiomyocyte hypertrophy. Circ. Res. **102:**959–965.

27. **Montagner, A., A. Yart, M. Dance, B. Perret, J. P. Salles, and P. Raynal.** 2005. A novel role for GAB1 and SHP2 in EGF-induced Ras activation. J. Biol. Chem. **280:**5350–5360.
28. **Morel, E., A. Marcantoni, M. Gastineau, R. Birkedal, F. Rochais, A. Garnier, A. M. Lompre, G. Vandecasteele, and F. Lezoualc'h.** 2005. cAMP-binding protein Epac induces cardiomyocyte hypertrophy. Circ. Res. **97:** 1296–1304.
29. **Nakamura, T., M. Colbert, M. Krenz, J. D. Molkentin, H. S. Hahn, G. W. Dorn II, and J. Robbins.** 2007. Mediating ERK 1/2 signaling rescues congenital heart defects in a mouse model of Noonan syndrome. J. Clin. Invest. **117:**2123–2132.
30. **Nissen, L. J., J. C. Gelly, and R. A. Hipskind.** 2001. Induction-independent recruitment of CREB-binding protein to the c-fos serum response element through interactions between the bromodomain and Elk-1. J. Biol. Chem. **276:**5213–5221.
31. **Oishi, K., H. Zhang, W. J. Gault, C. J. Wang, C. C. Tan, I. K. Kim, H. Ying, T. Rahman, N. Pica, M. Tartaglia, M. Mlodzik, and B. D. Gelb.** 2009. Phosphatase-defective LEOPARD syndrome mutations in PTPN11 have gain-of-function effects during Drosophila development. Hum. Mol. Genet. **18:**193–201.
32. **Pandit, B., A. Sarkozy, L. A. Pennacchio, C. Carta, K. Oishi, S. Martinelli, E. A. Pogna, W. Schackwitz, A. Ustaszewska, A. Landstrom, J. M. Bos, S. R. Ommen, G. Esposito, F. Lepri, C. Faul, P. Mundel, J. P. Lopez Siguero, R. Tenconi, A. Selicorni, C. Rossi, L. Mazzanti, I. Torrente, B. Marino, M. C. Digilio, G. Zampino, M. J. Ackerman, B. Dallapiccola, M. Tartaglia, and B. D. Gelb.** 2007. Gain-of-function RAF1 mutations cause Noonan and LEOPARD syndromes with hypertrophic cardiomyopathy. Nat. Genet. **39:** 1007–1012.
33. **Ramjaun, A. R., and J. Downward.** 2007. Ras and phosphoinositide 3-kinase: partners in development and tumorigenesis. Cell Cycle **6:**2902–2905.
34. **Roberts, A. E., T. Araki, K. D. Swanson, K. T. Montgomery, T. A. Schiripo, V. A. Joshi, L. Li, Y. Yassin, A. M. Tamburino, B. G. Neel, and R. S. Kucherlapati.** 2007. Germline gain-of-function mutations in SOS1 cause Noonan syndrome. Nat. Genet. **39:**70–74.
35. **Rosenberger, G., S. Meien, and K. Kutsche.** 2009. Oncogenic HRAS mutations cause prolonged PI3K signaling in response to epidermal growth factor in fibroblasts of patients with Costello syndrome. Hum. Mutat. **30:**352–362.
36. **Sampaio, C., M. Dance, A. Montagner, T. Edouard, N. Malet, B. Perret, A. Yart, J. P. Salles, and P. Raynal.** 2008. Signal Strength Dictates PI3K contribution to Ras/ERK1-2 activation via differential GAB1/SHP2 recruitment: consequences for resistance to EGFR inhibition. Mol. Cell. Biol. **28:**587–600.
37. **Sarkozy, A., C. Carta, S. Moretti, G. Zampino, M. C. Digilio, F. Pantaleoni, A. P. Scioletti, G. Esposito, V. Cordeddu, F. Lepri, V. Petrangeli, M. L. Dentici, G. M. Mancini, A. Selicorni, C. Rossi, L. Mazzanti, B. Marino, G. B. Ferrero, M. C. Silengo, L. Memo, F. Stanzial, F. Faravelli, L. Stuppia, E. Puxeddu, B. D. Gelb, B. Dallapiccola, and M. Tartaglia.** 2009. Germline BRAF mutations in Noonan, LEOPARD, and cardiofaciocutaneous syndromes: molecular diversity and associated phenotypic spectrum. Hum. Mutat. **30:**695–702.
38. **Schubbert, S., M. Zenker, S. L. Rowe, S. Boll, C. Klein, G. Bollag, I. van der Burgt, L. Musante, V. Kalscheuer, L. E. Wehner, H. Nguyen, B. West, K. Y. Zhang, E. Sistermans, A. Rauch, C. M. Niemeyer, K. Shannon, and C. P. Kratz.** 2006. Germline KRAS mutations cause Noonan syndrome. Nat. Genet. **38:**331–336.
39. **Shi, Z. Q., D. H. Yu, M. Park, M. Marshall, and G. S. Feng.** 2000. Molecular mechanisms for the SHP-2 tyrosine function in promoting growth factor stimulation of ERK activity. Mol. Cell. Biol. **20:**1526–1536.
40. **Tartaglia, M., S. Martinelli, L. Stella, G. Bocchinfuso, E. Flex, V. Cordeddu, G. Zampino, I. Burgt, A. Palleschi, T. C. Petrucci, M. Sorcini, C. Schoch, R. Foa, P. D. Emanuel, and B. D. Gelb.** 2006. Diversity and functional consequences of germline and somatic PTPN11 mutations in human disease. Am. J. Hum. Genet. **78:**279–290.
41. **Tartaglia, M., L. A. Pennacchio, C. Zhao, K. K. Yadav, V. Fodale, A. Sarkozy, B. Pandit, K. Oishi, S. Martinelli, W. Schackwitz, A. Ustaszewska, J. Martin, J. Bristow, C. Carta, F. Lepri, C. Neri, I. Vasta, K. Gibson, C. J. Curry, J. P. Siguero, M. C. Digilio, G. Zampino, B. Dallapiccola, D. Bar-Sagi, and B. D. Gelb.** 2007. Gain-of-function SOS1 mutations cause a distinctive form of Noonan syndrome. Nat. Genet. **39:**75–79.
42. **Uhlen, P., P. M. Burch, C. I. Zito, M. Estrada, B. E. Ehrlich, and A. M. Bennett.** 2006. Gain-of-function/Noonan syndrome SHP-2/Ptpn11 mutants enhance calcium oscillations and impair NFAT signaling. Proc. Natl. Acad. Sci. U. S. A. **103:**2160–2165.
43. **Wang, D., P. S. Chang, Z. Wang, L. Sutherland, J. A. Richardson, E. Small, P. A. Krieg, and E. N. Olson.** 2001. Activation of cardiac gene expression by myocardin, a transcriptional cofactor for serum response factor. Cell **105:** 851–862.
44. **Wang, S., W. M. Yu, W. Zhang, K. R. McCrae, B. G. Neel, and C. K. Qu.** 2009. Noonan syndrome/leukemia-associated gain-of-function mutations in SHP-2 phosphatase (PTPN11) enhance cell migration and angiogenesis. J. Biol. Chem. **284:**913–920.
45. **Wollert, K. C., T. Taga, M. Saito, M. Narazaki, T. Kishimoto, C. C. Glembotski, A. B. Vernallis, J. K. Heath, D. Pennica, W. I. Wood, and K. R. Chien.** 1996. Cardiotrophin-1 activates a distinct form of cardiac muscle cell hypertrophy. Assembly of sarcomeric units in series VIA gp130/leukemia inhibitory factor receptor-dependent pathways. J. Biol. Chem. **271:**9535–9545.
46. **Zhang, S. Q., W. G. Tsiaras, T. Araki, G. Wen, L. Minichiello, R. Klein, and B. G. Neel.** 2002. Receptor-specific regulation of phosphatidylinositol 3′-kinase activation by the protein tyrosine phosphatase SHP2. Mol. Cell. Biol. **22:**4062–4072.
47. **Zhang, S. Q., W. Yang, M. I. Kontaridis, T. G. Bivona, G. Wen, T. Araki, J. Luo, J. A. Thompson, B. L. Schraven, M. R. Philips, and B. G. Neel.** 2004. SHP2 regulates SRC family kinase activity and Ras/Erk activation by controlling Csk recruitment. Mol. Cell **13:**341–355.